



Efficient Coagulation Removal of Fluoride Using Lanthanum Salts: Distribution and Chemical Behavior of Fluorine

Xiacong Zhong^{1,2}, Chen Chen¹, Kang Yan¹, Shuiping Zhong¹, Ruixiang Wang^{1*} and Zhifeng Xu^{3*}

¹Faculty of Materials Metallurgy and Chemistry, Jiangxi University of Science and Technology, Ganzhou, China, ²State Key Laboratory of Separation and Comprehensive Utilization of Rare Metals, Guangzhou, China, ³Jiangxi College of Applied Technology, Ganzhou, China

OPEN ACCESS

Edited by:

Florent Allais,
AgroParisTech Institut des Sciences et
Industries du Vivant et de
L'environnement, France

Reviewed by:

Flemming Jappe Frandsen,
Technical University of Denmark,
Denmark
Hamid Rashidi Nodeh,
Standard Research Institute (SRI), Iran

*Correspondence:

Ruixiang Wang
jxustpaper@163.com
Zhifeng Xu
jxustzxf@163.com

Specialty section:

This article was submitted to
Green and Sustainable Chemistry,
a section of the journal
Frontiers in Chemistry

Received: 22 January 2022

Accepted: 14 February 2022

Published: 04 March 2022

Citation:

Zhong X, Chen C, Yan K, Zhong S,
Wang R and Xu Z (2022) Efficient
Coagulation Removal of Fluoride Using
Lanthanum Salts: Distribution and
Chemical Behavior of Fluorine.
Front. Chem. 10:859969.
doi: 10.3389/fchem.2022.859969

Abstract: La-loaded absorbents have been widely reported for fluoride removal due to the strong affinity of La^{3+} towards fluoride ion. Herein, chemical removal of fluoride from flue gas scrubbing wastewater using lanthanum salt is investigated. The retaining free F^- concentration, phase composition and morphology of filtration residues, and the distribution of fluorine have been investigated using ion-selective electrode, analytical balance, scanning electron microscopy, and X-ray diffractor. The results show that at La/F molar ratio $\geq 1:3.05$, the majority of fluorine exists as LaF_x^{3-x} complexes, leading to the failure of fluoride removal. At $1:3.20 \leq \text{La/F molar ratio} \leq 1:3.10$, the formation of LaF_3 is facilitated. However, co-existing LaF_x^{3-x} tends to absorb on the surface of LaF_3 particles, leading to the formation of colloidal solution with large numbers of $\text{LaF}_3 \cdot \text{LaF}_x^{3-x}$ suspended solids. At an optimized La/F molar ratio of 1:3.10, a fluoride removal of 97.86% is obtained with retaining fluorine concentration of 6.42 mg L^{-1} . Considering the existing of positively charged LaF_x^{3-x} and $\text{LaF}_3 \cdot \text{LaF}_x^{3-x}$, coagulation removal of fluoride is proposed and investigated using lanthanum salts and negatively charged $\text{SiO}_2 \cdot n\text{H}_2\text{O}$ colloidal particles, which is *in-situ* provided via Na_2SiO_3 hydrolysis at pH near 5.5. At a La/F molar ratio of 1:3.00 and Na_2SiO_3 dose of 0.50 g L^{-1} , a fluoride removal of 99.25% is obtained with retaining fluorine concentration of 2.24 mg L^{-1} . When Na_2SiO_3 dose increases to 1.00 g L^{-1} , the retaining fluorine concentration could be further reduced to 0.80 mg L^{-1} .

Keywords: fluoride removal, LaF_x^{3-x} complexes, coagulation, colloidal particles, precipitation

INTRODUCTION

Fluorine is one of the main contaminants in ground water and industrial effluents (Kong et al., 2020; Wan et al., 2021). Long-term intake of high-fluoride level water may lead to dental fluorosis, bone fluorosis and even neurological damage (Díaz-Flores et al., 2021). According to a standard issued by the World Health Organization (WHO), the fluorine content in drinking water should be less than 1.5 mg L^{-1} (Kim et al., 2020).

Following the large-scale exploitation of sphalerite ores in recent decades, the available sphalerite ores present a decreasing grade and contain complicated components (Hu et al., 2017). Among the typical impurities in sphalerite ores, the fluoride has attracted extensive attention due to its

detrimental effects on the peel-off of cathodic product (O'Keefe and Han, 1992) and the corrosion of lead-based anodes during the zinc electrowinning process (Zhong et al., 2015; Zhong et al., 2017). During the roasting of sphalerite ores, about 70% of the fluorine and chlorine in the ores enter the flue gas, and the others incorporate into the zinc calcine. In order to further reduce the content of fluorine and chlorine, the zinc calcine is usually treated in a rotary/tube furnace at elevated temperature, where fluorine and chlorine would be volatilized into flue gas in the form of HF and HCl, respectively (ÇinarŞahin et al., 2000; Kahvecioglu et al., 2013). Similarly, the zinc recovery processes from Waelz oxide, zinc oxide fumes, electric arc furnace dust, and other zinc-bearing dusts also discharge flue gas containing HF and HCl (Wei et al., 2010; Martins et al., 2021). During the scrubbing of above-mentioned flue gas, fluorine and chlorine transfer into the liquid phase, yielding a large amount of fluorine-containing acidic scrubbing wastewater. Due to the potential threat of fluorine on human's health, the fluoride ions must be selectively removed before being discharged. According to China's 'Emission Standard of Pollutants for Copper, Nickel and Cobalt Industries' (GB25467-2010), the fluoride ion content in discharge water should be below 5.0 mg L^{-1} (Liu., 2021).

Varied literatures have reported methods to efficiently remove fluoride from aqueous solutions, such as chemical precipitation (Turner et al., 2005; Chang and Liu., 2007; Huang et al., 2017), coagulation (Sandoval et al., 2019), adsorption (Ravuru et al., 2021; Yang et al., 2020; Sadhu et al., 2021), ion exchange (Samadi et al., 2014) and membrane separation (Feng et al., 2008; Arahmana et al., 2016). Among these methods, chemical precipitation has been widely used in metallurgical industry due to its advantages of simple operation, low cost, and applicability for high-fluorine wastewater. At present, the most widely used precipitant for fluoride removal is lime. However, due to the limitation of solubility product of CaF_2 , it is difficult to achieve a retaining fluoride content below 7.5 mg L^{-1} (Wajima et al., 2009) via lime precipitation, which is higher than the regulation limit of fluoride level.

As a highly electropositive metal, La^{3+} has a strong affinity towards fluoride ion (Nagaraj et al., 2017). Consequently, a large number of La-loaded absorbents have been reported for fluoride removal from ground water (G.J. Millar et al., 2017; Yan et al., 2017; Wang et al., 2018; He et al., 2019). Adsorption has been regarded as one of the most effective methods to treat ground water with relative low fluoride concentration ($<100 \text{ mg L}^{-1}$), which features low retaining fluoride concentration, low cost, and easy operation (Zhou et al., 2018). In a typical flue gas scrubbing wastewater, the fluoride content could be higher than 300 mg L^{-1} , La-loaded absorbents are not suitable to treat this aqueous solution because of its relatively small absorption capacity, which could lead to a large consumption of absorbents and long operation time. Hence, chemical precipitation of fluoride ion using lanthanum salt was proposed to remove fluoride in this work. In spite of extensive report on La-loaded absorbents, the distribution and chemical behavior of fluorine in the presence of La^{3+} remains unclear.

In the present work, the aqueous equilibrium diagrams of F- H_2O and La-F-Cl- H_2O systems were made to understand the species

TABLE 1 | Chemical reactions in La-F-Cl- H_2O aqueous system and their equilibrium constants.

Equation no	Reaction	Lg K
(1)	$2\text{H}^+ + 2\text{F}^- = \text{H}_2\text{F}_2$	6.77
(2)	$\text{H}^+ + \text{F}^- = \text{HF}$	3.18
(3)	$\text{H}^+ + 2\text{F}^- = \text{HF}_2^-$	3.62
(4)	$\text{La}^{3+} = \text{H}^+ + \text{La}(\text{OH})_2^+$	-8.66
(5)	$\text{La}^{3+} = 2\text{H}^+ + \text{La}(\text{OH})_2^+$	-18.14
(6)	$\text{La}^{3+} = 3\text{H}^+ + \text{La}(\text{OH})_3$	-27.91
(7)	$\text{La}^{3+} = 4\text{H}^+ + \text{La}(\text{OH})_4^-$	-40.86
(8)	$5\text{La}^{3+} = 9\text{H}^+ + \text{La}_5(\text{OH})_9^{6+}$	-71.20
(9)	$\text{La}^{3+} + \text{F}^- = \text{LaF}^{2+}$	3.85
(10)	$\text{La}^{3+} + 2\text{F}^- = \text{LaF}_2^+$	6.65
(11)	$\text{La}^{3+} + 3\text{F}^- = \text{LaF}_3$	8.69
(12)	$\text{La}^{3+} + 4\text{F}^- = \text{LaF}_4^-$	10.35
(13)	$\text{La}^{3+} + \text{Cl}^- = \text{LaCl}^{2+}$	0.29
(14)	$\text{La}^{3+} + 2\text{Cl}^- = \text{LaCl}_2^+$	-0.03
(15)	$\text{H}_2\text{O} = \text{H}^+ + \text{OH}^-$	-14.00

distribution of fluorine and lanthanum element in La-F-Cl- H_2O system at varied pH values. The retaining fluorine concentration, precipitate morphology and structure, and distribution of fluorine in La-F-Cl- H_2O system at different La/F molar ratios ($1:3.20 \leq \text{La}/\text{F}$ molar ratio $\leq 1:2.40$) were investigated and analyzed. Based on the experimental results mentioned above, the distribution and chemical behavior of fluorine in the presence of La^{3+} was discussed in detail. Furthermore, coagulation strategy was proposed to efficiently remove fluoride by adding Na_2SiO_3 and $\text{La}(\text{NO}_3)_3 \cdot \text{H}_2\text{O}$. The retaining fluorine in the equilibrium solution can be reduced to 0.80 mg L^{-1} .

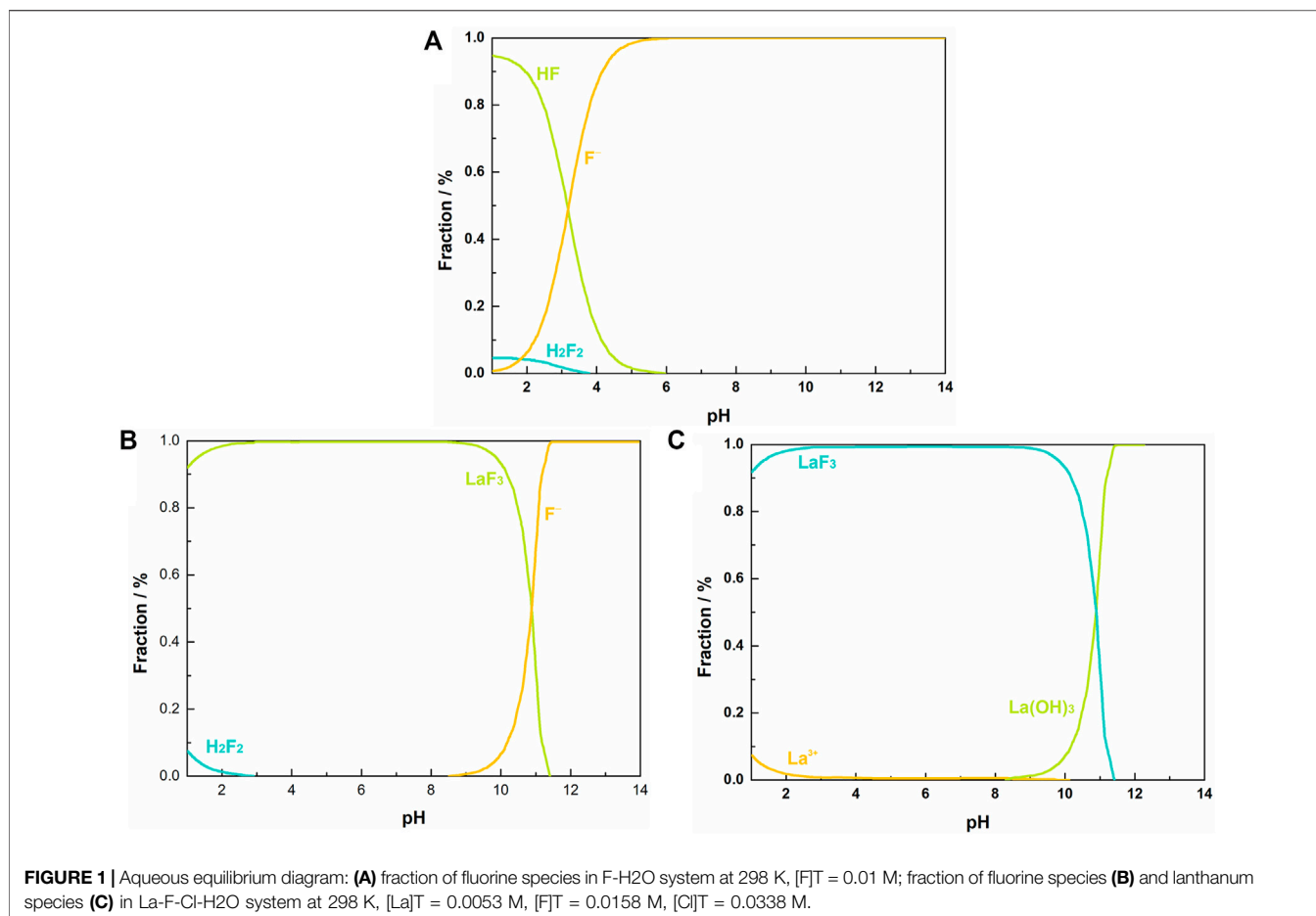
EXPERIMENTAL SECTION

Reagents

NaF, NaCl, $\text{La}(\text{NO}_3)_3 \cdot 6\text{H}_2\text{O}$, Na_2SiO_3 , NaOH, HNO_3 of analytical grade were purchased (Sinopharm Group, China) and used without further purification. The fluorine-containing synthetic solutions were prepared to stimulate flue gas scrubbing wastewater with NaF, NaCl, and deionized water, and its pH was adjusted to 2.0 ± 0.1 using HNO_3 . The fluorine and chlorine concentrations of synthetic solutions were set as 300 mg L^{-1} and $1,200 \text{ mg L}^{-1}$ respectively, closing to those of the industrial flue gas scrubbing wastewater.

Aqueous Equilibrium Diagram

The aqueous equilibrium diagrams of F- H_2O and La-F-Cl- H_2O systems were made using Hydra database and MEDUSA[®] software. Specifically, the Hydra database (Puigdomenech, 2004) provided thermodynamic data such as composition data, possible solid phases formed, potential chemical reactions and their equilibrium constants. In the F- H_2O system, the main species considered were HF, F, H_2F_2 , HF_2^- , H^+ and OH^- . In the La-F-Cl- H_2O system, F-, HF, H_2F_2 , HF_2^- , La^{3+} , LaF^{2+} , LaF_2^+ , LaF_3 , LaF_4^- , $\text{La}(\text{OH})_2^+$, $\text{La}(\text{OH})_3$, $\text{La}(\text{OH})_4^-$, $\text{La}_5(\text{OH})_9^{6+}$, LaCl^{2+} , LaCl_2^+ , H^+ and OH^- were taken into account. The chemical reactions and corresponding equilibrium constants are listed in **Table 1**. These data were sent to MEDUSA[®] software to make



diagrams based on principles of mass conservation, simultaneous chemical equilibrium, and electronic charge neutrality. The distribution of fluorine species in the F-H₂O system, and the distribution of La or F species in the La-F-Cl-H₂O system were analyzed.

Experimental Procedure and Characterization

The pH of the fluorine-containing synthetic solution was firstly adjusted to 5.5 ± 0.1 using NaOH. Afterwards, different amounts of La(NO₃)₃·6H₂O were added to 200 ml of synthetic solution under agitation (200 rpm) based on a specific La/F molar ratio. The fluoride removal reaction proceeded for 1 h at $30 \pm 1^\circ\text{C}$. During the reaction, fluoride ion selective electrode and pH meter were used to monitor the variation of pF ($-\log(a_{\text{F}^-})$, measured continuously without pH adjustment) and pH value with reaction time. At the end of reaction, the solution was vacuum filtered using inorganic filtration membrane (pore diameter of 0.22 μm, Jinteng®). The filtration time was recorded, and the filtration residue was collected. The final pF of the solution was measured using ion selective electrode after adjusting the pH of filtrate to 5.5 ± 0.1 . The filtration residues collected were dried overnight in an oven at 80°C. After this, the weights of filtration residues were

obtained using weight loss method. The morphologies and phase structures of filtration residues were investigated using scanning electron microscopy (SEM, MIRA 3) and X-ray diffraction (XRD, MiniFlex 600-C). At a La/F molar ratio $\geq 1:3.05$, there was no precipitate obtained, extra NaF (0.133 g) was added into the filtrate to produce LaF₃ precipitates, which were further collected, dried, weighed and analyzed as mentioned above.

Removal of fluoride from synthetic solution using Na₂SiO₃ and La³⁺ was also investigated. Firstly, different doses of Na₂SiO₃ (0.25–1.00 g L⁻¹) were added into the synthetic solution under agitation (200 rpm). After 30 min of agitation, the solution pH was adjusted to 5.5 ± 0.1 . Then La(NO₃)₃·6H₂O was added to target a La/F molar ratio of 1:3.00. After 1 h of reaction, the solution was vacuum filtered. The filtration residue and filtrate were analyzed as mentioned above. To confirm the presence or absence of LaF_x^{3-x} or LaF₃·LaF_x^{3-x}, extra NaF (0.133 g) was added to the filtrate, and whether precipitate formed was checked.

RESULTS AND DISCUSSION

Aqueous Equilibrium Diagram

Figure 1A shows the distribution of fluorine species in F-H₂O equilibrium system. At pH < 4.0, fluorine element exists in the form

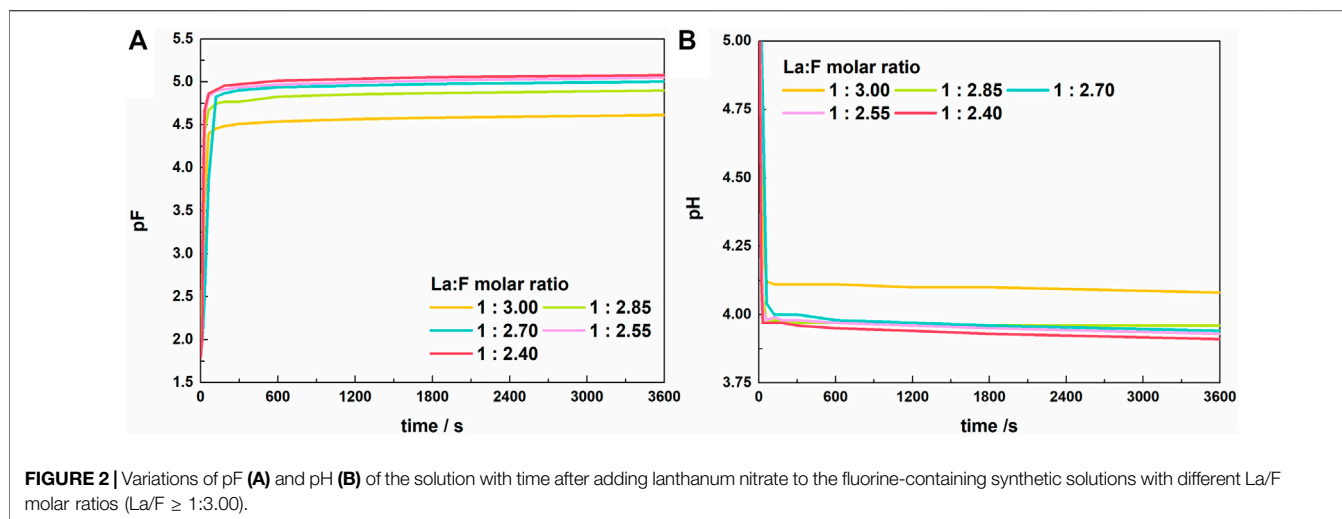


FIGURE 2 | Variations of pF (A) and pH (B) of the solution with time after adding lanthanum nitrate to the fluorine-containing synthetic solutions with different La/F molar ratios ($\text{La}/\text{F} \geq 1:3.00$).

of HF, F^- and H_2F_2 . The proportion of H_2F_2 decreases as pH increases from 1.0 to 4.0 and descends to zero at $\text{pH} > 4.0$. As a weak acid, most of fluorine exists as HF at low pH range (Li et al., 2013). Over the pH range 1.0–5.5, the proportion of HF descends rapidly as pH increases, while the proportion of F^- exhibits a reverse variation. At $\text{pH} > 5.5$, HF becomes negligible, and almost all the fluorine exists as free F^- . **Figures 1B, C** show the distribution of F and La species in La-F-Cl- H_2O equilibrium system. The molar ratio of La/F in the system is set as 1:3.00, and the total concentration of F and Cl is 0.0158 and 0.0338 M, respectively, same as the synthetic solution. As shown in **Figures 1B,C**, at $\text{pH} < 3.0$, a small part of fluorine exists as H_2F_2 , while the majority of fluorine exists as LaF_3 . Over the pH range 3.0–8.3, almost all fluorine exists in the form of LaF_3 . Interestingly, as pH further increases (> 8.3), La^{3+} tends to hydrolyze to $\text{La}(\text{OH})_3$, resulting in a decrease of LaF_3 proportion. Based on the thermodynamic diagrams of La-F-Cl- H_2O equilibrium system, it can be confirmed that at acidic environment ($\text{pH} < 3.0$), part of fluorine exists in the form of H_2F_2 , which could hinder the combination of fluorine with La^{3+} . Nevertheless, in the pH range over 8.3, La^{3+} hydrolysis reaction would compete with LaF_3 precipitation reaction, resulting in a low fluoride removal and a high retaining fluoride concentration. Therefore, the pH range for fluoride removal using La^{3+} should be controlled between 5.5 and 8.3. Given the pH of the synthetic solution is about 2.0, in order to reduce the neutralization cost, the pH for fluoride removal is optimized to 5.5. Similarly, several literatures have also reported the largest adsorption capacity and highest defluorination efficiency of La-loaded adsorbents near pH of 5.5 (Cai et al., 2018).

Fluoride Removal at La/F Molar Ratios $\geq 1:3.00$

Figure 2 shows the variation of solution pF and pH with time during the reaction at La/F molar ratios $\geq 1:3.00$. At the initial stage, pF increased rapidly, indicating a sharp decreasing of free F^- concentration (**Figure 2A**). Meanwhile, the solution pH value exhibits a quick drop (**Figure 2B**). The decreasing pH could be explained by the enhanced ionization of HF due to the decreasing

concentration of free F^- , which results in a larger H^+ activity. When the reaction time exceeds 300 s, the solution pF and pH change slightly, suggesting an equilibrium state obtained between La^{3+} and fluorine species. As the La/F molar ratio increases from 1:3.00 to 1:2.85, the stable pF increases apparently, and the pH exhibits a reverse change. This result indicates that addition of excessive La^{3+} can promote the combination of F^- and La. However, when the La/F molar ratio further increases, the stable pF increases slightly, indicating that increasing lanthanum dose has a small effect on the stable pF at La/F molar ratio $\geq 1:2.85$.

As mentioned above, during the fluoride removal at La/F molar ratios $\geq 1:3.00$, the stable pF is larger than 4.5, namely, the free F^- concentration could be reduced to below 0.5 mg L^{-1} . However, after 1 h of reaction the solutions with La/F molar ratios $\geq 1:3.00$ remained clear and transparent (shown in **Supplementary Figure S1**). During the vacuum filtration using inorganic membranes with a pore diameter of $0.22 \mu\text{m}$, the mass of filtration residue collected from five solutions with different La/F molar ratios ($\geq 1:3.00$) is neglectable.

Due to the low free F^- concentration and the absence of precipitate, it is reasonable to assume that most of fluorine retains in the solution as soluble species. In order to verify this assumption, extra NaF (0.133 g) was added to each solution. The digital photos of solutions after adding extra NaF are shown in **Supplementary Figure S1**. Interestingly, flocculent precipitates formed immediately upon the addition of extra NaF. The XRD pattern and SEM image of the precipitates are shown in **Supplementary Figure S2**. It is apparent that characteristic peaks of LaF_3 are observed in the XRD pattern of the precipitates (**Supplementary Figure S2A**), signifying the formation of LaF_3 with extra addition of NaF. As shown in **Supplementary Figure S2B**, LaF_3 precipitates exist as irregular crystalline bulks and amorphous particles simultaneously. The crystalline bulks may be resulted from the recrystallization of amorphous floccules during the vacuum filtration and drying process (Hermans and Weidinger, 1946). The mass of precipitates formed by adding extra NaF in different solutions is shown in **Supplementary Figure S3**. It is found that the mass of

TABLE 2 | Distribution of fluoride element in aqueous solutions with La/F molar ratio $\geq 1:3$ after reaction for 1 h.

La/F molar ratio	Free F ⁻			LaF _x ^{3-x}		Retaining fluoride ^c mg L ⁻¹	Removal %
	C ^a /mg L ⁻¹	Mass/mg	Proportion/%	Mass ^b /mg	Proportion/%		
1:3.00	0.45	0.090	0.15	59.910	99.85	300	0
1:2.85	0.26	0.052	0.09	59.948	99.91	300	0
1:2.70	0.20	0.040	0.07	59.960	99.93	300	0
1:2.55	0.18	0.036	0.06	59.964	99.94	300	0
1:2.40	0.16	0.032	0.05	59.968	99.95	300	0

^aCalculated with final pF of filtrate measured at pH 5.5 ± 0.1 .

^bCalculated with the fluorine balance ($60 \text{ mg} - \text{mass}_{\text{free F}^-} - \text{mass}_{\text{filtration residues}} \times \frac{57}{196}$).

^cIncluding free F⁻ and LaF_x^{3-x}.

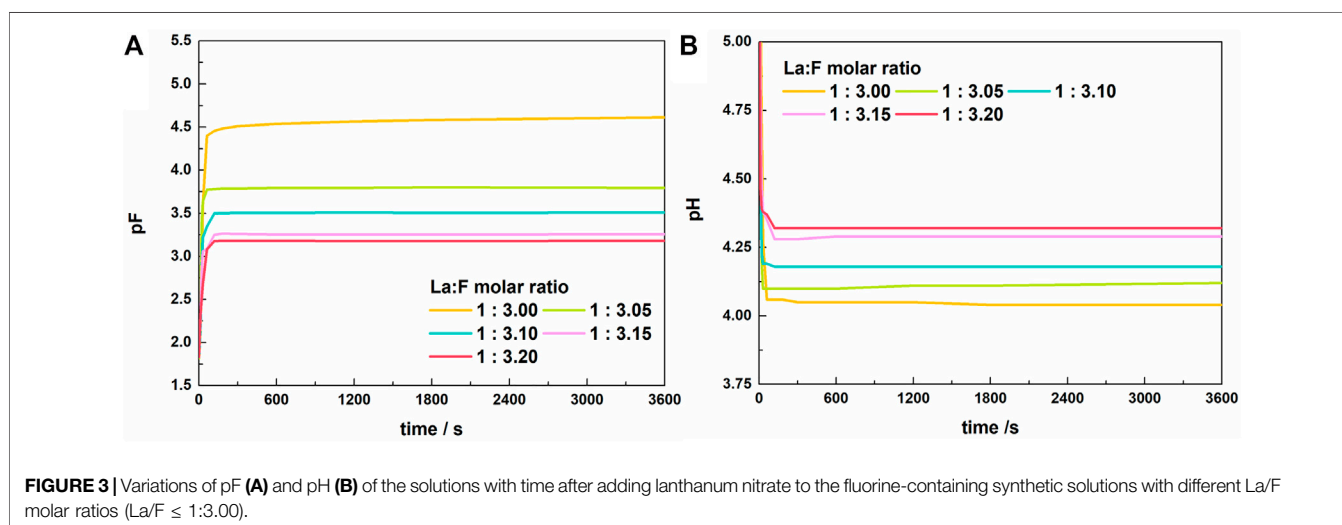


FIGURE 3 | Variations of pF (A) and pH (B) of the solutions with time after adding lanthanum nitrate to the fluoride-containing synthetic solutions with different La/F molar ratios (La/F $\leq 1:3.00$).

precipitates is close to the theoretical LaF₃ production. These results confirm that at La/F molar ratio $\geq 1:3.00$, fluorine retains in the solution as soluble species. However, reducing the La/F molar ratio by adding extra NaF could facilitate the formation of LaF₃.

Considering the fact that fluoride ion could complex La³⁺, which results in the formation of LaF²⁺ and LaF₂⁺, it could be inferred that in aqueous solutions with La/F molar ratios $\geq 1:3.00$, most of fluorine retains in solution as LaF_x^{3-x} complexes. Similarly, Antuñano et al. (2016) and Liu et al. (2020) reported the presence of AlF_n³⁻ⁿ complexes in Al-F-H₂O system. Table 2 shows the distribution of fluorine in the solution after 1 h of reaction with La/F molar ratios $\geq 1:3.00$. It could be found that over 99% fluorine retains in solution as LaF_x^{3-x}. As the La/F molar ratio increases, the proportion of LaF_x^{3-x} slightly increases. Since all fluorine retains in the solution in the form of LaF_x^{3-x} or free F⁻, the fluoride removal efficiencies of solutions with La/F molar ratios $\geq 1:3.00$ are all zero.

Fluoride Removal at La/F Molar Ratios $\leq 1:3.00$

It is confirmed that at La/F molar ratios $\geq 1:3.00$ the fluorine could be not removed in the form of LaF₃ precipitates. Therefore, it is necessary to investigate the chemical behavior of fluorine at La/F molar ratios $\leq 1:3.00$.

Figure 3 shows the variation of pF and pH with time in solutions with La/F molar ratios $\leq 1:3.00$. Similar to the results obtained in solutions with La/F molar ratios $\geq 1:3.00$, the reaction between La³⁺ and fluorine get an equilibrium state in 5 min. The stable pF decreases as the La/F molar ratio decreases, while the final pH shows the reverse change. Notably, at La/F molar ratio $\leq 1:3.00$, the La/F molar ratio has a more significant influence on the stable pH and pF of the solutions. Specifically, as La/F molar ratio decreases from 1:3.00 to 1:3.05, the stable pF decreases from 4.50 to 3.75, indicating a much higher concentration of free F⁻ retaining in the solution.

Supplementary Figure S4 shows the photos of the solutions with different La/F molar ratios ($\leq 1:3.00$) after 1 h of reaction. It is apparent that a large number of white floccules suspend in the solutions with La/F molar ratios $\leq 1:3.05$. As La/F molar ratio decreases, the solution becomes more and more turbid. It is worth noting that after standing for 2 h, the suspended solids could not settle. Therefore, it can be inferred that colloidal solutions were formed at La/F molar ratio $\leq 1:3.05$. The formation of colloidal solution could be explained as follows. As mentioned above, in solutions at La/F $\geq 1:3.00$, the insufficient fluorine results in formation of LaF_x^{3-x}, such as LaF²⁺ and LaF₂⁺. In solution of La/F $\leq 1:3.05$, the presence of sufficient fluorine promotes the formation of LaF₃. However, the coexisting LaF_x^{3-x} tends to adsorb on the surface of LaF₃, resulting in negative charges on

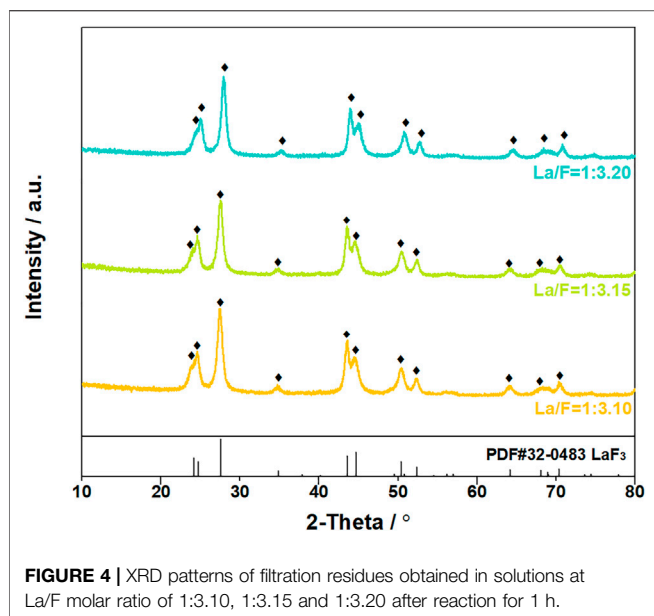


FIGURE 4 | XRD patterns of filtration residues obtained in solutions at La/F molar ratio of 1:3.10, 1:3.15 and 1:3.20 after reaction for 1 h.

the surface of suspended solids ($\text{LaF}_3 \cdot \text{LaF}_x^{3-x}$). This would enhance the stability of suspended solids and result in the formation of a colloidal solution.

The suspended solids were collected by vacuum filtration using inorganic membrane. Interestingly, filtration residues could only be obtained from solutions with La/F molar ratio $\leq 1:3.10$. The XRD patterns and SEM images of the filtration residues obtained from solutions with La/F molar ratio of 1:3.10, 1:3.15 and 1:3.20 are shown in **Figures 4, 5**, respectively. It can be found that the main phase of the filtration residues obtained in three solutions is LaF_3 . There is no other apparent characteristic

peak, signifying the high purity of LaF_3 precipitates. As shown in **Figure 5**, the LaF_3 residues presents two kinds of structures, part of LaF_3 exists as irregular bulks with high crystalline, while the others exhibit amorphous structures. As La/F molar ratio decreases, excessive fluoride accelerates the formation of LaF_3 , resulting in smaller particle size and a larger crystalline degree of LaF_3 . It is noteworthy that, at La/F molar ratio of 1:3.15 and 1:3.20, the filtrate obtained in vacuum filtration remains light pale, suggesting a small number of suspended solids remain in the solution. This could be explained with the smaller size of colloid particles formed with large fluoride excess coefficient, which could not be intercepted by the filtrate cake and membrane.

Table 3; Figure 6 show the distribution of fluorine in solutions with La/F molar ratios $\leq 1:3.00$ after 1 h of reaction. It could be found that, as La/F molar ratio decreases (the excess coefficient of fluoride increases), the free F^- concentration of the equilibrium solution increases. At La/F molar ratio of 1:3.00 and 1:3.05, no fluorine is removed from the solution in the form of filtration residues, and over 98% fluorine retains in solution as LaF_x^{3-x} or $\text{LaF}_3 \cdot \text{LaF}_x^{3-x}$. Remarkably, at La/F molar ratio of 1:3.10, about 97.86% fluorine is removed from the aqueous system in the form of filtration residue, and the retaining fluoride concentration is about 6.42 mg L^{-1} , slightly higher than the emission standard established in GB25467-2010. As La/F molar ratio further decreases, the proportion of free F^- increases obviously, while the proportion of filtration residues decreases, resulting in a higher retaining free F^- concentration and a decreasing fluoride removal efficiency. Specifically, when La/F molar ratio increases to 1:3.20, the retaining fluoride concentration is about 32.16 mg L^{-1} , much higher than the emission standard. Although the presence of excess fluoride could facilitate the precipitation of LaF_3 , it leads to a significant increase in the retaining free F^- concentration and fine suspended colloid particles

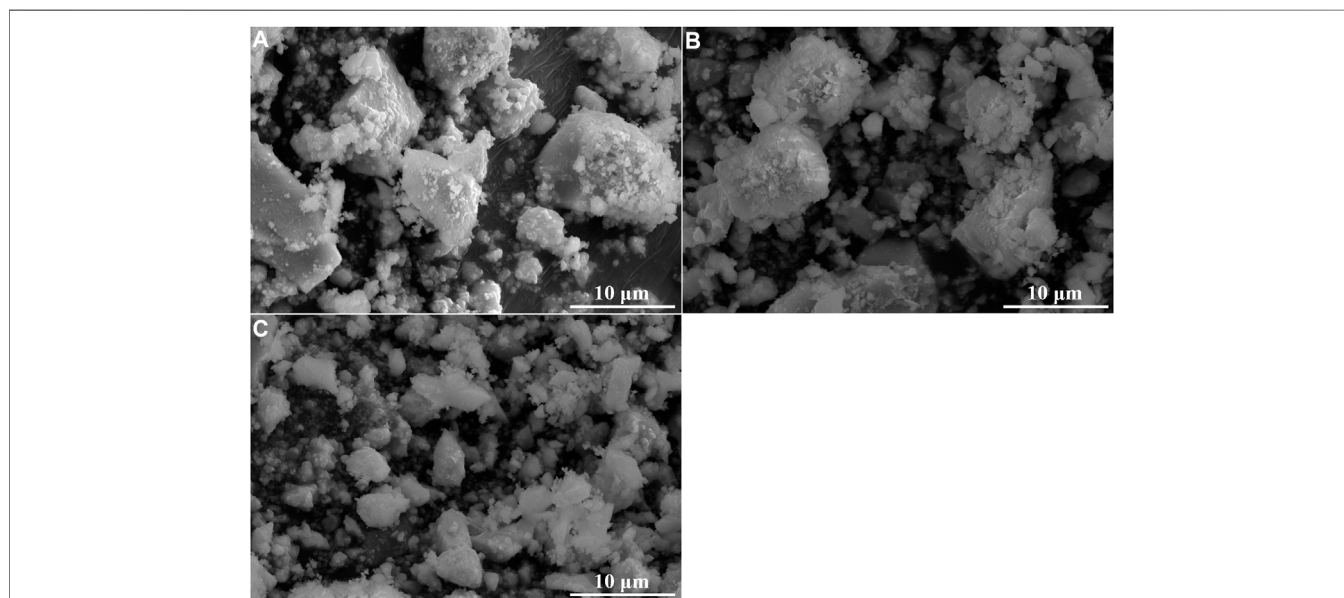


FIGURE 5 | SEM images of filtration residues obtained in solutions with La/F molar ratios of 1:3.10 (A), 1:3.15 (B) and 1:3.20 (C) after reaction for 1 h.

TABLE 3 | Distribution of fluorine element in aqueous solutions with La/F molar ratios $\leq 1:3.00$ after reaction for 1 h.

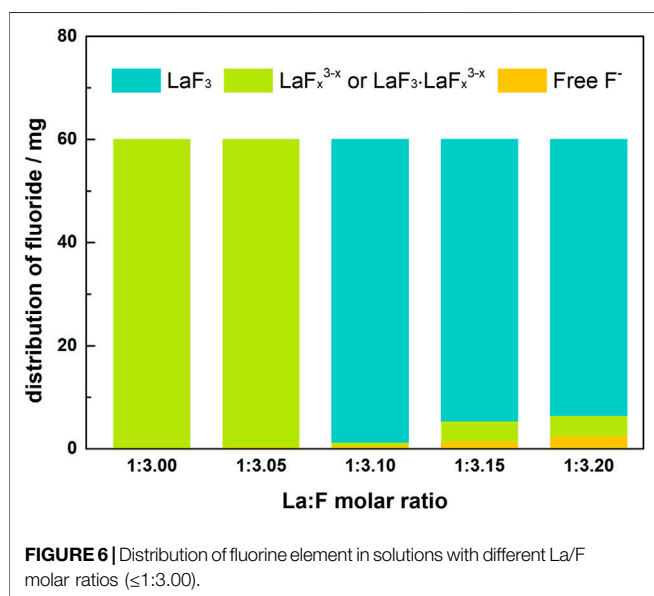
La/F molar ratio	Free F ⁻			LaF _x ^{3-x} or fine LaF ₃ ·LaF _x ^{3-x}		Filtration residues			Retaining fluoride ^d	Removal
	C ^a (mg L ⁻¹)	Mass (mg)	(%)	Mass ^b (mg)	(%)	Mass ^c (mg)	Filtration time (min)	(%)	mg L ⁻¹	%
1:3.00	0.51	0.10	0.17	59.90	99.83	0	-	0	300	0
1:3.05	1.19	0.24	0.40	59.76	98.60	0	-	0	300	0
1:3.10	3.30	0.66	1.10	0.62	1.03	58.72	158	97.86	6.42	97.86
1:3.15	7.14	1.43	2.38	3.98	6.63	54.59	95	90.98	27.06	90.98
1:3.20	12.35	2.47	4.12	3.96	6.60	53.57	76	89.28	32.16	89.28

^acalculated with final pH of filtrate measured at pH 5.5 ± 0.1.

^bcalculated with the fluorine balance ($60 \text{ mg} - \text{mass}_{\text{free F}^-} - \text{mass}_{\text{filtration residues}} \times \frac{57}{196}$).

^ccalculated with the mass of precipitate ($\text{mass}_{\text{filtration residues}} \times \frac{57}{196}$) based on the assumption that precipitate contains LaF₃ only.

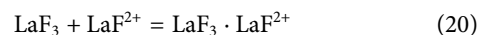
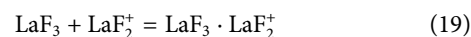
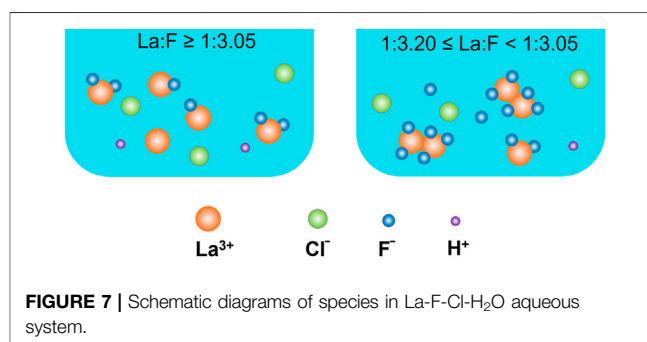
^dincluding free F⁻, LaF_x^{3-x} and fine LaF₃·LaF_x^{3-x}.



(LaF₃·LaF_x^{3-x}). Therefore, the La/F molar ratio is optimized as 1:3.10 for precipitating fluoride using lanthanum salts.

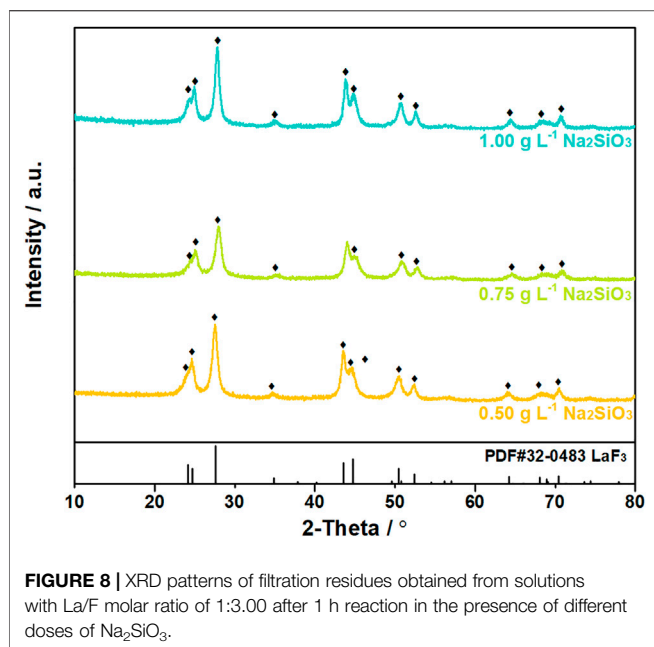
Chemical Reactions Between F⁻ and La³⁺

Based on the above results, it can be found that the chemical reactions between F⁻ and La³⁺ are sensitive to the La/F molar ratio. As shown in **Figure 7**, at La/F molar ratio $\geq 1:3.05$, the fluoride is relatively insufficient, there is not enough fluoride participate in the precipitation reaction (**Eq. 16**), resulting in the formation of LaF₂⁺ (**Eq. 17**), or even LaF₂²⁺ (**Eq. 18**). Under this condition, although the free F⁻ concentration in the aqueous system can be reduced to a very low level, most of fluoride retains in the solution in the form of LaF_x^{3-x} complexes, resulting in the failure of fluoride removal. At $1:3.20 \leq \text{La:F} < 1:3.05$, sufficient fluoride enhances the precipitation of LaF₃. However, coexisting LaF_x^{3-x} in the aqueous solution could adsorb on the surface of LaF₃, resulting in the formation of colloidal solution with LaF₃·LaF_x^{3-x} suspended solids (**Eqs 19–20**).



Coagulation Removal of Fluoride Using La³⁺ and Na₂SiO₃

At the optimized La/F molar ratio of 1:3.10, the retaining fluoride concentration in the filtrate is 6.42 mg L⁻¹, exceeding the emission standard level (GB25467-2010). Therefore, chemical precipitation using lanthanum salt fails to sufficiently remove fluoride from aqueous solution. Given that fluoride could exist in the form of positively charged LaF_x^{3-x} or LaF₃·LaF_x^{3-x} ($x = 1$ or 2), SiO₂· n H₂O, as a well-known negatively charged colloidal particle (Lin et al., 2018), is introduced to facilitate the coagulation of LaF_x^{3-x} and LaF₃·LaF_x^{3-x} based on electrostatic interaction. In practice, Na₂SiO₃ was firstly added into the synthetic solution. After 0.5 h of agitation, the solution pH was adjusted to 5.5 ± 0.1 to produce active colloidal particles (SiO₂· n H₂O) *in situ*. Afterwards, the lanthanum salt is added to target a La/F molar ratio of 1:3.00, rather than 1:3.10 in order to reducing the retaining free F⁻ concentration.



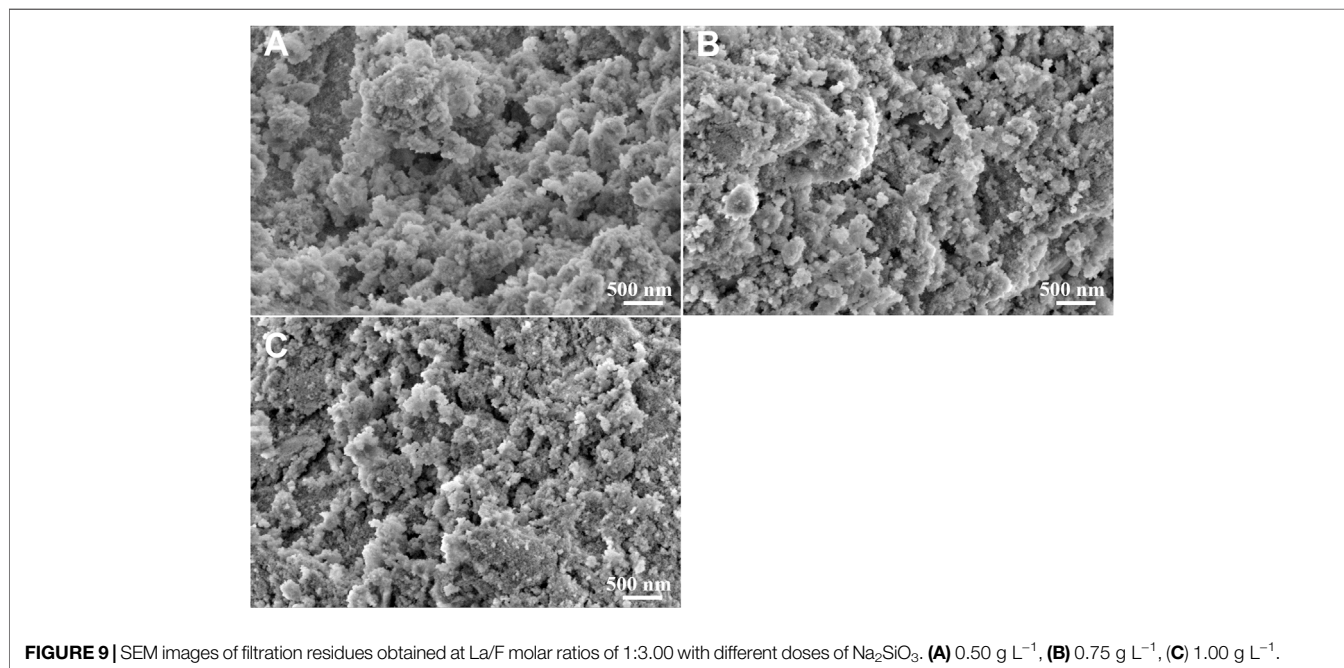
Supplementary Figure S5 shows the digital photos of solutions with different doses of Na₂SiO₃ after 1 h of reaction. In the absence of Na₂SiO₃ (**Supplementary Figure S5A**), the solution remains clear and transparent. Correspondingly, during the vacuum filtration, there is no filtration residues obtained from this solution. In the presence of 0.25 g L⁻¹ Na₂SiO₃ (**Supplementary Figure S5B**), about 0.10 g L⁻¹ filtration residues were collected from the solution. As Na₂SiO₃ dose further increases, the solutions at equilibrium state become more and more turbid, signifying the formation of suspended

particles. Consequently, much more filtration residues were obtained from these solutions.

The XRD patterns and SEM images of the filtration residues were shown in **Figures 8, 9**. In the XRD patterns of filtration residues obtained from solutions with 0.50–1.00 g L⁻¹ Na₂SiO₃, only the featured peaks of LaF₃ appears, demonstrating the main phase of the filtration residues is LaF₃. The absence of characteristic peaks of SiO₂ may be explained by the low content of SiO₂·*n*H₂O or the amorphous structure of SiO₂·*n*H₂O. The morphologies of filtration residues obtained with Na₂SiO₃ addition are shown in **Figure 9**. It can be found that the presence of Na₂SiO₃ has an obvious effect on the structures of filtrate residues. A large number of fine irregular particles agglomerates, resulting in the lumps in large size (≥5 μm). However, the dose of Na₂SiO₃ does not show obvious influence on the morphologies of filtration residues.

Figure 10 shows the distribution of F, Si and La element on the surface of filtration residues obtained from solution with La/F molar ratio of 1:3.00 and 0.50 g L⁻¹ Na₂SiO₃. It is observed that the F and La element is uniformly distributed on the surface of filtration residues, further demonstrating the formation of LaF₃ precipitates. In spite of the absence of featured peaks of SiO₂ in the XRD pattern, the Si element is detected on the surface of filtration residues, which testifies the participation of colloidal particles (SiO₂·*n*H₂O) in the coagulation of LaF₃. The EDS results indicate that the contents of Si in filtration residues are 2.87 wt%, 3.67 wt% and 4.25 wt%, corresponding to the addition of 0.50 g L⁻¹, 0.75 g L⁻¹, and 1.00 g L⁻¹ Na₂SiO₃, respectively.

Table 4; Figure 11 shows the distribution of fluorine element in solutions with La/F molar ratio of 1:3.00 and different doses of Na₂SiO₃. In the absence of Na₂SiO₃, even though free F⁻ concentration could be reduced to 0.51 mg L⁻¹, nearly 99.83% fluorine retains in the solution as LaF_{*x*}^{3-*x*}. When Na₂SiO₃ dose



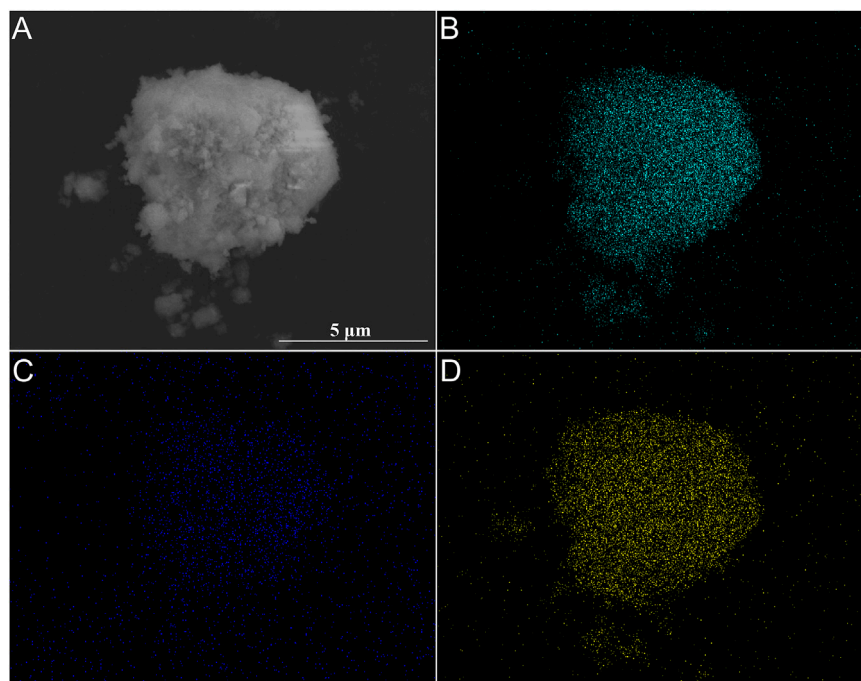


FIGURE 10 | SEM image (A) and elements mapping (B–D) of filtration residues obtained at La/F molar ratios of 1:3.00 in the presence of $0.50 \text{ g L}^{-1} \text{ Na}_2\text{SiO}_3$. (B) F, (C) Si, (D) La.

TABLE 4 | Distribution of fluorine element in aqueous solutions (La/F molar ratio = 1:3.00) after 1 h of reaction in the presence of Na_2SiO_3 .

Na_2SiO_3 dose (g L^{-1})	Free F^-			LaF_x^{3-x} or fine $\text{LaF}_3\text{LaF}_x^{3-x}$		Filtration residues			Retaining fluoride ^d	Removal
	C ^a (mg L^{-1})	Mass (mg)	(%)	Mass (mg)	(%)	Mass (mg)	Filtration time (min)	(%)	(mg L^{-1})	%
0	0.51	0.10	0.17	59.90 ^b	99.83	0	-	0	300.00	0
0.25	1.89	0.38	0.63	47.55 ^b	79.25	12.07	2.3	20.12	271.15	20.12
0.50	2.24	0.45	0.75	0	0	59.55 ^c	340	99.25	2.24	99.25
0.75	2.33	0.47	0.78	0	0	59.53 ^c	362	99.22	2.33	99.22
1.00	0.80	0.16	0.27	0	0	59.84 ^c	325	99.73	0.80	99.73

^acalculated with final pF of filtrate measured at $\text{pH } 5.5 \pm 0.1$.

^bCalculated with the fluorine balance ($60 \text{ mg} - \text{mass}_{\text{free F}^-} - \text{mass}_{\text{filtration residues}} \times \frac{57}{190}$) based on the assumption that precipitate contains LaF_3 only (Si is neglected).

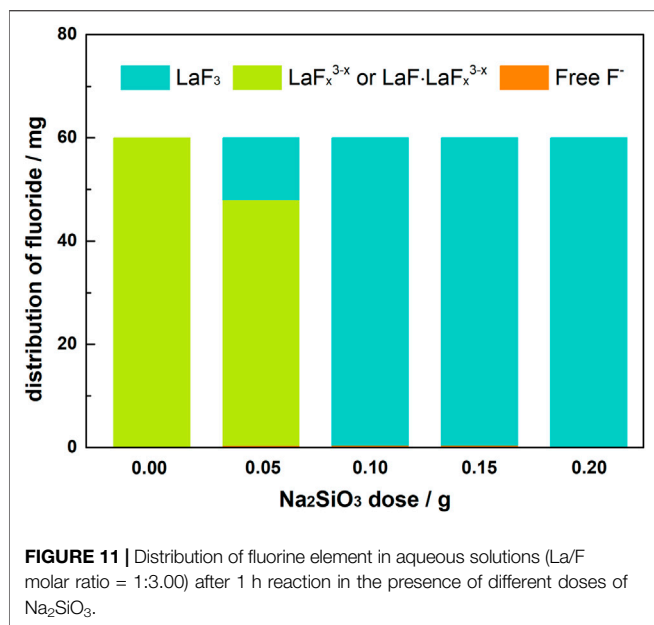
^cCalculated with the fluorine balance ($60 \text{ mg} - \text{mass}_{\text{free F}^-}$), the absence of LaF_x^{3-x} or $\text{LaF}_3\text{LaF}_x^{3-x}$ is proved by adding extra NaF.

^dIncluding free F^- , LaF_x^{3-x} and fine $\text{LaF}_3\text{LaF}_x^{3-x}$.

reaches 0.25 g L^{-1} , about 20.12% fluorine is removed from the solution in the form of filtration residues, and 79.25% remains in the solution in the form of LaF_x^{3-x} . As Na_2SiO_3 dose increases to 0.50 g L^{-1} , a fluorine removal efficiency of 99.25% could be obtained. When adding extra NaF into the filtrate, the solution keeps clear and transparent, proving the absence of LaF_x^{3-x} or $\text{LaF}_3\text{LaF}_x^{3-x}$. The retaining fluoride concentration in equilibrium solution is 2.24 mg L^{-1} , lower than the emission standard established in GB25467-2010. As Na_2SiO_3 dose further increases, the fluorine removal efficiency ascends slightly, and the retaining fluoride concentration could be reduced to 0.8 mg L^{-1} , lower than the limited fluoride level established by

the WHO. However, it is noteworthy that, at a Na_2SiO_3 dose $\geq 0.50 \text{ g L}^{-1}$, the filtration time is longer than 5 h, which could be explained by the formation of a large amount of sticky $\text{SiO}_2 \cdot n\text{H}_2\text{O}$ colloidal particles.

Above results verify our assumption that the presence of negatively charged $\text{SiO}_2 \cdot n\text{H}_2\text{O}$ colloidal particles could interact with positively charged LaF_x^{3-x} and $\text{LaF}_3\text{LaF}_x^{3-x}$, promoting their aggregation and settlement. It is demonstrated that coagulation removal of fluoride could be achieved through adding Na_2SiO_3 and lanthanum salts. However, the presence of $\text{SiO}_2 \cdot n\text{H}_2\text{O}$ colloidal particles render the difficulty in solid/liquid separation, the operation parameters for coagulation



removal of fluoride using Na₂SiO₃ and lanthanum salts should be optimized in future works.

CONCLUSION

Pyrometallurgical treatment of low-grade sphalerite ores and zinc-bearing dusts discharges a large amount of flue gas containing HF and HCl. During the flue gas scrubbing step, fluorine and chlorine transfer into the liquid phase, yielding a large amount of fluorine-containing scrubbing wastewater. In this work, precipitation removal and coagulation removal of fluoride from flue gas scrubbing wastewater (300 mg L⁻¹ fluoride) using lanthanum salt is investigated.

The chemical reaction between La³⁺ and F⁻ has been discussed based on the distribution of fluorine in solutions with different La/F molar ratios. At acidic environment (pH ≤ 4.0), part of fluorine exists as HF and H₂F₂, retarding the combination of La³⁺ and fluorine. Nonetheless, at pH > 8.3, La³⁺ hydrolysis reaction would compete with LaF₃ precipitation reaction, resulting in a low fluoride removal. Consequently, the pH for fluoride removal is optimized to 5.5. At La/F molar ratio ≥ 1:3.05, most of fluorine retains in the solution in the form of LaF_x^{3-x} complexes, resulting in the failure of fluoride removal. At 1:3.20 ≤ La:F ratio < 1:3.05, sufficient fluoride enhances the precipitation of LaF₃. However, LaF_x^{3-x} coexisting in the aqueous solution could adsorb on the surface of LaF₃, resulting in the formation of colloidal solution with large numbers of LaF₃·LaF_x^{3-x} suspended solids. In summary, at optimized La/F molar ratio of 1:3.10, about 97.86% fluoride is removed from the aqueous system in the form of filtration residue, and the retaining fluoride concentration is about 6.42 mg L⁻¹, slightly higher than the emission standard established in GB25467-2010.

Considering the existing of positively charged LaF_x^{3-x} and LaF₃·LaF_x^{3-x}, coagulation removal of fluoride is proposed and investigated using lanthanum salts and negatively charged

SiO₂·nH₂O colloidal particles (*in-situ* produced *via* Na₂SiO₃ hydrolysis at pH near 5.5). At a La/F molar ratio of 1:3.00 and Na₂SiO₃ dose of 0.50 g L⁻¹, a fluoride removal of 99.25% is obtained with retaining fluorine concentration of 2.24 mg L⁻¹. When Na₂SiO₃ dose increases to 0.20 g, the retaining fluorine concentration could be further reduced to 0.80 mg L⁻¹, lower than the limited fluoride level established by the WHO. During the coagulation removal of fluoride using lanthanum salts and Na₂SiO₃, the presence of SiO₂·nH₂O colloidal particles render the difficulty in solid/liquid separation, the operation parameters for coagulation removal of fluoride should be optimized in future works.

Generally, coagulation removal of fluoride has a huge potential to be adopted in metallurgical industry due to high removal efficiency, low consumption of lanthanum salts, and relative low cost of lanthanum salts and Na₂SiO₃. However, the influence of impurities, especially anions such as SO₄²⁻, Cl⁻, CO₃²⁻, and NO₃⁻, on the chemical behavior and distribution of fluoride during coagulation removal of fluoride should be fully evaluated before industrialized application of this process.

DATA AVAILABILITY STATEMENT

The original contributions presented in the study are included in the article/**Supplementary Material**, further inquiries can be directed to the corresponding authors.

AUTHOR CONTRIBUTIONS

RW: Writing review and editing, Funding acquisition. CC: Investigation, Writing original draft. XZ: Supervision, Methodology, Formal analysis, Writing review and editing. KY: Validation. SZ: Resources, Formal analysis. ZX: Supervision, Writing review and editing.

FUNDING

This work was financially supported by the National Key Research and Development Program of China (2019YFC1908405); Natural Science Foundation of Jiangxi Province (Youth Program; 20202BAB214015); Training plan for academic and technical leaders of major disciplines in Jiangxi Province (Youth Program; 20212BCJ23006, 20212BCJL23052); Program of Qingjiang Excellent Young Talents, Jiangxi University of Science and Technology (JXUSTQJYX2020015); Research Fund of State Key Laboratory of Rare Metals Separation and Comprehensive Utilization (GK-201905), China; Distinguished Professor Program of Jinggang Scholars in institutions of higher learning, Jiangxi Province.

SUPPLEMENTARY MATERIAL

The Supplementary Material for this article can be found online at: <https://www.frontiersin.org/articles/10.3389/fchem.2022.859969/full#supplementary-material>

REFERENCES

- Antuñano, N., Cambra, J. F., and Arias, P. L. (2016). Fluoride Removal from Double Leached Waelz Oxide Leach Solutions as Alternative Feeds to Zinc Calcine Leaching Liquors in the Electrolytic Zinc Production Process. *Hydrometallurgy* 161, 65–70. doi:10.1016/j.hydromet.2016.01.008
- Arahmana, N., Mulyati, S., Lubis, M. R., Takagi, R., and Matsuyama, H. (2016). The Removal of Fluoride from Water Based on Applied Current and Membrane Types in Electrodialysis. *J. Fluorine Chem.* 19197, 102. doi:10.1016/j.jfluchem.2016.10.002
- Cai, J., Zhao, X., Zhang, Y., Zhang, Q., and Pan, B. (2018). Enhanced Fluoride Removal by La-Doped Li/Al Layered Double Hydroxides. *J. Colloid Interf. Sci.* 509, 353–359. doi:10.1016/j.jcis.2017.09.038
- Chang, M. F., and Liu, J. C. (2007). Precipitation Removal of Fluoride from Semiconductor Wastewater. *J. Environ. Eng.* 133 (4), 419–425. doi:10.1061/(asce)0733-9372(2007)133:4(419)
- Çınarşahin, F., Derin, B., and Yücel, O. (2000). Chloride Removal from Zinc Ash. *Scand. J. Metall.* 29 (5), 224. doi:10.1034/j.1600-0692.2000.d01-26.x
- Díaz-Flores, P., Arcibar-Orozco, J., Flores-Rojas, A., and Rangel-Méndez, J. (2021). Synthesis of a Chitosan-Zeolite Composite Modified with La(III): Characterization and its Application in the Removal of Fluoride from Aqueous Systems. *Water Air Soil Poll* 232, 235. doi:10.1007/s11270-021-05185-1
- Feng, C., Khulbe, K. C., Matsuura, T., Gopal, R., Kaur, S., Ramakrishna, S., et al. (2008). Production of Drinking Water from saline Water by Air-gap Membrane Distillation Using Polyvinylidene Fluoride Nanofiber Membrane. *J. Membr. Sci.* 311 (1-2), 1. doi:10.1016/j.memsci.2007.12.026
- He, Y., Zhang, L., An, X., Wan, G., Zhu, W., and Luo, Y. (2019). Enhanced Fluoride Removal from Water by Rare Earth (La and Ce) Modified Alumina: Adsorption Isotherms, Kinetics, Thermodynamics and Mechanism. *Sci. Total Environ.* 688, 184–198. doi:10.1016/j.scitotenv.2019.06.175
- Hermans, P. H., and Weidinger, A. (1946). On the Recrystallization of Amorphous Cellulose. *J. Am. Chem. Soc.* 68 (12), 2547–2552. doi:10.1021/ja01216a037
- Hu, X., Peng, X., and Kong, L. (2017). Removal of Fluoride from Zinc Sulfate Solution by *In Situ* Fe(III) in a Cleaner Desulfuration Process. *J. Clean. Prod.* 164, 163–170. doi:10.1016/j.jclepro.2017.06.213
- Huang, H., Liu, J., Zhang, P., Zhang, D., and Gao, F. (2017). Investigation on the Simultaneous Removal of Fluoride, Ammonia Nitrogen and Phosphate from Semiconductor Wastewater Using Chemical Precipitation. *Chem. Eng. J.* 307, 696–706. doi:10.1016/j.cej.2016.08.134
- Kahvecioglu, Ö., Derin, B., and Yücel, O. (2013). Carbothermal Recovery of Zinc from Brass Ash. *Mineral. Process. Extractive Metall.* 112 (2), 95–101. doi:10.1179/037195503225002790
- Kim, M., Choong, C. E., Hyun, S., Park, C. M., and Lee, G. (2020). Mechanism of Simultaneous Removal of Aluminum and Fluoride from Aqueous Solution by La/Mg/Si-Activated Carbon. *Chemosphere* 253, 126580. doi:10.1016/j.chemosphere.2020.126580
- Kong, L., Tian, Y., Pang, Z., Huang, X., Li, M., Li, N., et al. (2020). Needle-like Mg-La Bimetal Oxide Nanocomposites Derived from Periclase and Lanthanum for Cost-Effective Phosphate and Fluoride Removal: Characterization, Performance and Mechanism. *Chem. Eng. J.* 382, 122963. doi:10.1016/j.cej.2019.122963
- Li, J., Zhou, Z., Yang, T., and Chen, L. (2013). Thermodynamics of Fluoride Removal from Waste Acid in Metallurgy Plant. *J. Cent. South. Univ. (Sci. Tech.)* 44 (9), 3580. in Chinese.
- Lin, M., Pei, Z., Lei, S., Liu, Y., Xia, Z., and Xie, F. (2018). Trace Muscovite Dissolution Separation from Vein Quartz by Elevated Temperature and Pressure Acid Leaching Using Sulphuric Acid and Ammonia Chloride Solutions. *Physicochem. Probl. Mi.* 54, 448. doi:10.5277/ppmp1839
- Liu, J., Yin, Z., Liu, W., Li, X., and Hu, Q. (2020). Treatment of Aluminum and Fluoride during Hydrochloric Acid Leaching of Lepidolite. *Hydrometallurgy* 191, 105222. doi:10.1016/j.hydromet.2019.105222
- Liu, S. (2021). Practical Study on the Advanced Defluorination Process Optimization of Copper Smelting Wastewater. *Indust. Water Treat.* 41 (1), 118. in Chinese. doi:10.1016/j.jwpe.2021.101998
- Martins, J. M. A., Dutra, A. J. B., Mansur, M. B., and Guimarães, A. S. (2021). Comparison of Oxidative Roasting and Alkaline Leaching for Removing Chloride and Fluoride from Brass Ashes. *Hydrometallurgy* 202, 105619. doi:10.1016/j.hydromet.2021.105619
- Millar, G. J., Couperthwaite, S. J., Wellner, D. B., Macfarlane, D. C., and Dalzell, S. A. (2017). Removal of Fluoride Ions from Solution by Chelating Resin with Imino-Diacetate Functionality. *J. Water Process Eng.* 20, 113–122. doi:10.1016/j.jwpe.2017.10.004
- Nagaraj, A., Sadasivuni, K. K., and Rajan, M. (2017). Investigation of Lanthanum Impregnated Cellulose, Derived from Biomass, as an Adsorbent for the Removal of Fluoride from Drinking Water. *Carbohydr. Polym.* 176, 402–410. doi:10.1016/j.carbpol.2017.08.089
- O'Keefe, T. J., and Han, J. (1992). Electrochemical Evaluation of Adherence of Zinc to Aluminium Cathodes. *Surf. Coating Technol.* 53 (3), 231. doi:10.1016/0257-8972(92)90381-J
- Puigdomenech, I. (2004). *Make Equilibrium Diagrams Using Sophisticated Algorithms (MEDUSA)*, *Inorganic Chemistry*. Stockholm, Sweden: Royal Institute of Technology.
- Ravuru, S. S., Jana, A., and De, S. (2021). Performance Modeling of Layered Double Hydroxide Incorporated Mixed Matrix Beads for Fluoride Removal from Contaminated Groundwater with the Scale up Study. *Separat. Purif. Technol.* 277, 119631. doi:10.1016/j.seppur.2021.119631
- Sadhu, M., Bhattacharya, P., Vithanage, M., and Padmaja Sudhakar, P. (2021). Adsorptive Removal of Fluoride Using Biochar - A Potential Application in Drinking Water Treatment. *Separat. Purif. Technol.* 278, 119106. doi:10.1016/j.seppur.2021.119106
- Samadi, M. T., Zarrabi, M., Sepehr, M. N., Ramhormozi, S. M., Azizian, S., and Amrane, A. (2014). Removal of Fluoride Ions by Ion Exchange Resin: Kinetic and Equilibrium Studies. *Environ. Eng. Manage. J.* 13, 205. doi:10.1016/j.ecolecon.2013.11.002
- Sandoval, M. A., Fuentes, R., Nava, J. L., Coreño, O., Li, Y., and Hernández, J. H. (2019). Simultaneous Removal of Fluoride and Arsenic from Groundwater by Electrocoagulation Using a Filter-Press Flow Reactor with a Three-Cell Stack. *Separat. Purif. Technol.* 208, 208–216. doi:10.1016/j.seppur.2018.02.018
- Turner, B. D., Binning, P., and Stipp, S. L. S. (2005). Fluoride Removal by Calcite: Evidence for Fluorite Precipitation and Surface Adsorption. *Environ. Sci. Technol.* 39 (24), 9561–9568. doi:10.1021/es0505090
- Wajima, T., Umetsu, Y., Narita, S., and Sugawara, K. (2009). Adsorption Behavior of Fluoride Ions Using a Titanium Hydroxide-Derived Adsorbent. *Desalination* 249, 323–330. doi:10.1016/j.desal.2009.06.038
- Wan, K., Huang, L., Yan, J., Ma, B., Huang, X., Luo, Z., et al. (2021). Removal of Fluoride from Industrial Wastewater by Using Different Adsorbents: A Review. *Sci. Total Environ.* 773, 145535. doi:10.1016/j.scitotenv.2021.145535
- Wang, J., Wu, L., Li, J., Tang, D., and Zhang, G. (2018). Simultaneous and Efficient Removal of Fluoride and Phosphate by Fe-La Composite: Adsorption Kinetics and Mechanism. *J. Alloys Compd.* 753, 422–432. doi:10.1016/j.jallcom.2018.04.177
- Wei, J., Zhang, Z., Jiang, F., Fan, G., and Chen, Y. (2010). Speciation Analysis of the Fluoride in the Smelting Flue Gas of Copper and Nickel Metallurgy. *J. Tsinghua Sci. Technol.* 50 (12), 1925–1929. in Chinese. doi:10.1016/S1872-5813(11)60001-7
- Yan, L., Tu, H., Chan, T., and Jing, C. (2017). Mechanistic Study of Simultaneous Arsenic and Fluoride Removal Using Granular TiO₂-La Adsorbent. *Chem. Eng. J.* 313, 983–992. doi:10.1016/j.cej.2016.10.142
- Yang, K., Li, Y., Tian, Z., Peng, K., and Lai, Y. (2020). Removal of Fluoride Ions from ZnSO₄ Electrolyte by Amorphous Porous Al₂O₃ Microfiber Clusters: Adsorption Performance and Mechanism. *Hydrometallurgy* 197, 05455. doi:10.1016/j.hydromet.2020.105455
- Zhong, X., Wang, R., Xu, Z., Jiang, L., Lv, X., Lai, Y., et al. (2017). Influence of Mn²⁺ on the Performance of Pb-Ag Anodes in Fluoride/chloride-Containing H₂SO₄ Solutions. *Hydrometallurgy* 174, 195–201. doi:10.1016/j.hydromet.2017.10.014
- Zhong, X., Yu, X., Jiang, L., Lv, X., Liu, F., Lai, Y., et al. (2015). Influence of Fluoride Ion on the Performance of Pb-Ag Anode during Long-Term Galvanostatic Electrolysis. *Jom* 67 (9), 2022–2027. doi:10.1007/s11837-015-1550-1

Zhou, J., Zhu, W., Yu, J., Zhang, H., Zhang, Y., Lin, X., et al. (2018). Highly Selective and Efficient Removal of Fluoride from Ground Water by Layered Al-Zr-La Tri-metal Hydroxide. *Appl. Surf. Sci.* 435, 920–927. doi:10.1016/j.apsusc.2017.11.108

Conflict of Interest: The authors declare that the research was conducted in the absence of any commercial or financial relationships that could be construed as a potential conflict of interest.

Publisher's Note: All claims expressed in this article are solely those of the authors and do not necessarily represent those of their affiliated organizations, or those of

the publisher, the editors, and the reviewers. Any product that may be evaluated in this article, or claim that may be made by its manufacturer, is not guaranteed or endorsed by the publisher.

Copyright © 2022 Zhong, Chen, Yan, Zhong, Wang and Xu. This is an open-access article distributed under the terms of the Creative Commons Attribution License (CC BY). The use, distribution or reproduction in other forums is permitted, provided the original author(s) and the copyright owner(s) are credited and that the original publication in this journal is cited, in accordance with accepted academic practice. No use, distribution or reproduction is permitted which does not comply with these terms.